Proc. of the 8th International Conference NEET 2013, Zakopane, Poland, June 18–21, 2013

Effect of Thermal Treatment on the Structure and Mechanical Properties of Coatings Based on (Ti, Hf, Nb, Si)N

A.D. Pogrebnjak[a,*], F.F. Komarov[b], O.V. Sobol[c], A.Sh. Kaverina[a], A.P. Shypylenko[a] and C. Karwat[d]

[a]Sumy State University, Rymskogo-Korsakova 2, Sumy, 40007, Ukraine
[b]Belarus State University, Minsk, Belarus
[c]National Technical University "KhPi", Kharkov, Ukraine
[d]Lublin University of Technology, Lublin, Poland

Current paper presents the results of investigating of nanostructured cathode arc vacuum evaporation coatings, based on (Ti, Hf, Nb, Si)N. Several methods of the structural and elemental analysis were used: proton microbeam, nano- and micro-electron beam, X-ray diffraction analysis. To determine tribological properties (scratch resistance, adhesive and cohesive strength) of the coatings, scratch testing were conducting. Influence of thermal annealing at temperatures 300, 500, 800, 1000 °C on elemental composition, microstructure, residual stress, phase composition, profiles of atomic distribution in the coatings were investigated.

DOI: 10.12693/APhysPolA.125.1312
PACS: 61.46.−w, 62.20.Qp, 62.25.−g

1. Introduction

Multicomponent and nanostructured coatings nowadays are one of the most promising protective materials because of their high hardness, high abrasion, corrosion and fatigue resistance as well as high temperature of oxidation, etc. [1–10]. It is well known that binary — TiN, CrN, MoN, triple — TiNAl, TiCrN [11–14] and quaternary — Ti–Zr–Si–N, Ti–Hf–Si–N compounds are commonly used for wear protection, corrosion protection, and possess high thermal stability even up to 900–1000 °C [5, 6, 9].

Recently published works (e.g. [9]) have shown that nanostructured (nanocomposite) (Ti–Hf–Si–N) coatings, obtained by C-PVD method may have two phases: (Ti, Hf)N — solid solution phase and α-Si_3N_4 — amorphous phase. At the same time these coatings exhibit high hardness up to 48 GPa (superhardness), along with low friction coefficient of 0.12 to 0.45 and thermal stability up to 900 °C. Therefore, it is of particular interest to add to such system Nb, which has (as Hf) a high enthalpy of mixing, for improving the resistance to high temperature oxidation and possibly to improve other physical and mechanical properties of coatings such as abrasion resistance and elastic modulus.

For providing of studies multielement coatings (Ti, Hf, Nb, Si)N were selected. According to the proposed and experimentally proven concept of high entropy multicomponent alloys such coatings are able to significantly improve thermal stability of the material [1]. Therefore, the creation of new types of nanocomposite (nanostructured) coatings on the base of (Ti, Hf, Nb, Si)N by means of cathode arc vacuum evaporation (CAVE) and subsequent study of their physical and mechanical properties is an important task of modern materials science.

2. Experiments

A cathode-arc-vacuum-evaporation "Bulat-6" with HF generator [3, 5] was applied. Potential bias was applied to the substrate from the HF generator of pulsed damped oscillations with a frequency of < 1 MHz. The duration of each pulse was of 60 μs, with a repetition rate of ≈ 10 kHz. The amount of negative self-bias potential of the substrate caused by HF diode effect was 2.3 kV. A constant negative potential $U_s = (-40 \div 200)$ V was applied to the substrate, the residual gas pressure was 0.0066 Pa and arc current did not exceed 85 A.

Cathodes of the multicomponent alloys (Ti, Hf, Nb, Si)N were prepared by vacuum-arc melting in an atmosphere of high purity argon.

The elemental composition was studied using scanning electron microscope (SEM) with energy dispersive X-ray (EDX) microanalysis (JEOL-7000F, Japan). The Rutherford backscattering (RBS) method with He^+ ions of 1.7 MeV (the scattering angle was $\theta = 170°$) was used to perform the element analysis over a sample depth.

The phase composition and structural studies were performed on the X-ray diffractometer DRON-3M and Rigaku RINT-2500 — MDG Japan, in the filtered radiation of Cu K_α using in the secondary beam graphite monochromator. In order to study the stress-strain state of the coatings, the method of X-ray strain measurements ("α-$\sin^2\phi$" method) and its modifications were used, which are commonly applied to the coatings with strong axial texture [10–14].

The distribution of elements in nanostructured coatings has been studied by micro-proton beam induced X-ray emission (μ-PIXE) measurements at an initial particle energy of 1.4 MeV (IAPC, Sumy).

To determine tribological properties of coatings the scratch tester REVETEST (CSM Instruments) [6] was

*corresponding author; e-mail: alexp@i.ua

used. Simultaneously the power of acoustic emission, friction coefficient and the penetration depth of the indenter and the value of the normal load (F_N) were recorded. Three scratches were applied to each sample using diamond spherical indenter "Rockwell C".

Tests were carried out under the following conditions: the load on the indenter increased from 0.9 to 70 N, speed of the indenter movement was 1 mm/min, scratch length — 10 mm, the loading rate — 6.91 N/min, the frequency of a digital signal — 60 Hz, acoustic emission — 9 Db. Tests determined the minimum (critical) load L_{C1}, which corresponds to the beginning of the indenter penetration into the coating; L_{C2} — top when the first cracks appear; L_{C3} — the peel of some parts of coating; L_{C4} — plastic abrasion of the coating to the substrate. The deformation of the coating by the diamond indenter was investigated further using the integrated optical microscope and electron-ion scanning microscope Quanta 200 3D, equipped with an integrated system of Pegasus 2000 for microanalysis.

3. Experimental results and discussions

Before turning to the analysis of X-ray data, it should be noted that, for understanding of the sequence of processes occurring in the surface region during the deposition, it is necessary to compare the heat of formation of possible nitrides.

In accordance with [7], the enthalpies of formation (ΔH) of the four binary nitrides are shown in Table I. It means that the heat of formation of all systems is a relatively large and negative, indicating that there is a high probability of the formation of such systems through the transfer of material from the target to the substrate.

TABLE I

The enthalpies of formation (ΔH) of the binary nitrides.

	TiN	HfN	NbN	Si_3N_4
ΔH [KJ/mol]	−337.7	−373	−234.7	−738.1

TABLE II

Crystallite size and the lattice period for different temperatures of annealing.

No.	Annealing temperature [°C]	a [nm]	Crystallite size [nm]
1	300	0.43440	5.0
3	500	0.44398	5.9
4	800	0.43520	6.4
2	1000	0.42752	7.7

In this case, the proximity of the values of the heat of formation of TiN and HfN, NbN (Table II) creates conditions for the formation of sufficiently homogeneous solid solution (Ti, Hf, Nb)N. Thus, such element as Nb, which stabilize the bcc lattice, and refractory composites of Hf and Ti (due to their high affinity for nitrogen) have crucial effect on formation of a nitride phase in high entropy one-component alloy.

Figure 1 and Table II show the results of X-ray diffraction study. The first annealing (Fig. 1, curve 2) leads to an abrupt relaxation of compressive stresses, which is accompanied by a decrease of lattice period in direction perpendicular to the plane of growth. This annealing leads to a considerable recrystallization processes. Then, annealing up to 800 °C (Fig. 1, curve 4) has practically no effect on the stress state, leaving period of lattice the same. A significant relaxation processes were detected after annealing up to 1000 °C, which leads to the sharp decrease of the lattice period in the direction perpendicular to the plane of growth. At the same time the average size of the crystallites are exposed to the increase throughout the all temperature range of annealing and reaches maximum size of 7.7 nm at 1000 °C, i.e. increases for more than 60% compared to the initial state.

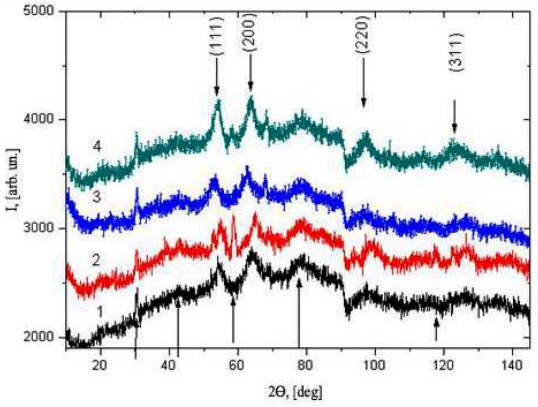

Fig. 1. Diffraction spectra of coatings obtained by GXRD: 1 — as deposited, 2 — annealed at 1000 °C, 3 — annealed at 500 °C, 4 — annealed at 800 °C. The lower arrows indicate the peaks from substrate, the upper arrows indicate peaks of coating.

Research of the surface morphology of (Ti, Hf, Nb, Si)N coatings showed that the surface coating has some drops components (Fig. 2). It is known [6] that the coatings deposited at different pressures of nitrogen have different level of internal stress: high microhardness is usually accompanied by higher internal stresses that actively relax.

The following Fig. 3a shows the energy spectra of backscattered $^4He^+$, obtained from samples coated with (Ti, Hf, Nb, Si)N on a steel substrate.

As it is seen from Fig. 3a, the concentration of Ti, Hf, Nb, Si elements after annealing at $T = 500$ °C and 800 °C is comparable to concentration of these elements before annealing, which indicates the uniformity of distribution of elements through the thickness of the coating. Annealing of samples up to 1000 °C for 30 min led to formation of oxide film on the coating surface and to redistribution of the elements in the form of films. Calculation of element distribution over depth for the spectra 1 and 4, indicated in Fig. 3a are shown in Fig. 3b and c. As it is seen from the profile elements distribution in the depth of the coat-

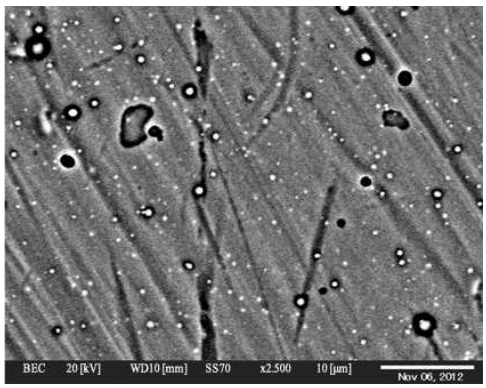

Fig. 2. SEM image of nanocomposite combined coatings surface.

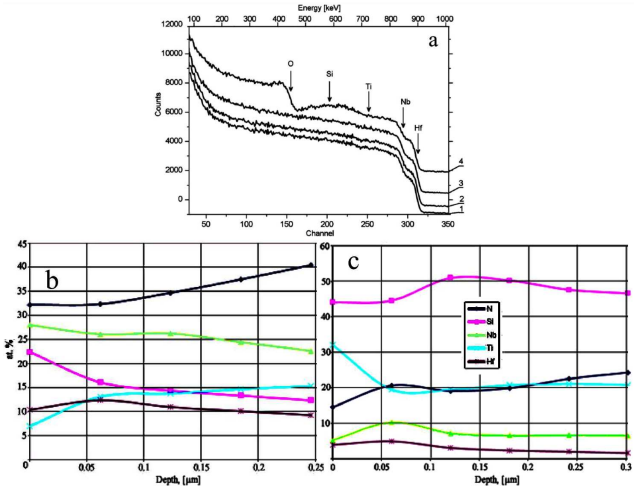

Fig. 3. (a) Energy RBS spectra obtained for coatings (Ti, Hf, Nb, Si)N, at the initial state and after annealing at $T = 500\,^{\circ}\mathrm{C}$, $800\,^{\circ}\mathrm{C}$, $1000\,^{\circ}\mathrm{C}$ for 30 min in air. Calculation of element distribution over depth of for the coatings (Ti, Hf, Nb, Si)N: (b) at the initial state, (c) after annealing at $T = 1000\,^{\circ}\mathrm{C}$.

ing (Fig. 3b, c) the concentration of the elements near the surface (in the depth) is almost constant (Fig. 3b). Annealing to $1000\,^{\circ}\mathrm{C}$ (Fig. 3c) leads to a slight change in the concentration of elements, in particular near the surface, and the appearance of the oxide film, with thickness 70 nm.

Preliminary results obtained by μ-PIXE microbeam in depth and on the surface of nanostructured coatings showed that the annealing to $800\,^{\circ}\mathrm{C}$ leads to the segregation of impurities (for example, the elements Hf and Nb) in nanograins. A siliconitride layer which is formed as a result of the thermal diffusion of Si along nanograin boundaries leads to the formation of SiN_x — amorphous phase.

Figure 4a shows the results of tests performed on the scratch tester REVETEST of sample (Ti–Hf–Nb–Si)N at the minimum (critical) load $L_{C1} = 2.46$ N and at the load at which the first cracks appear $L_{C2} = 10.25$ N.

It should be noted that when the load increases, the

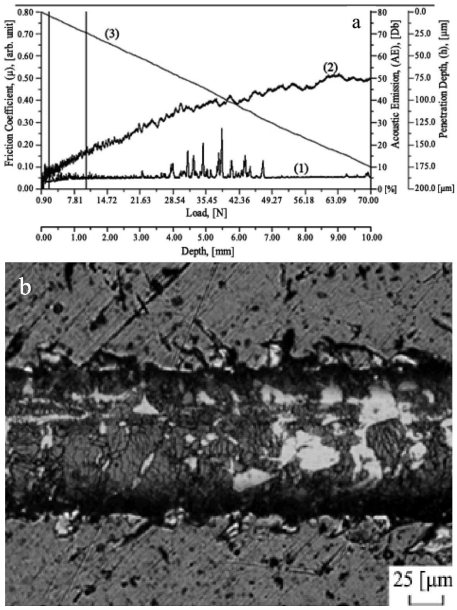

Fig. 4. Results of adhesion of tests system coatings (Ti, Hf, Nb, Si)N steel substrate: (a) dependence AE (1), friction coefficient μ (2), and the depth of penetration (3) and (b) structure of the coating in the fracture zone at loads in the range 0.9–90.0 N.

curve describing the dependence of friction coefficient on the load gets an oscillatory character. The increase of the friction coefficient is accompanied by a surge of acoustic emission. The above described behavior of all recorded parameters in these experiments (coefficient of friction, hardness) shows that the hard coating with thickness of ≤ 1 μm deposited on a surface of softer material (steel) shows a substantial resistance to diamond indenter to almost its full abrasion under high loads [15–17].

When testing coatings it can be can clearly distinguished different threshold values of critical load which lead to different types of destruction. What is more only a minimum (critical) L_{C1} load and a load at which the first crack appears L_{C2} can be associated with the adhesive destruction of coatings.

Destruction of the coating begins with the appearance of chevron cracks at the bottom of wear groove, which causes the increase of local stresses and friction. This leads to the subsequent rapid abrasion of coating (Fig. 4b) [18, 19].

According to the results of adhesion tests, cohesive destruction of the coatings (as-deposited) (Ti–Hf–Nb–Si)N appears at the minimal (critical) load $L_{C1} = 2.38$ N and adhesion destruction occurs at a load when the first crack appears $L_{C2} = 9.81$ N. Figure 5a–c shows the results of scratch tests of samples after annealing at 500, 800 and $1000\,^{\circ}\mathrm{C}$. According to obtained results it can be argued that the greatest resistance to wear is demonstrated by coatings after high-temperature annealing up $1000\,^{\circ}\mathrm{C}$ (lowest takeout of coating material (c)). Accordingly, the degree of wear resistance decreases with decreasing

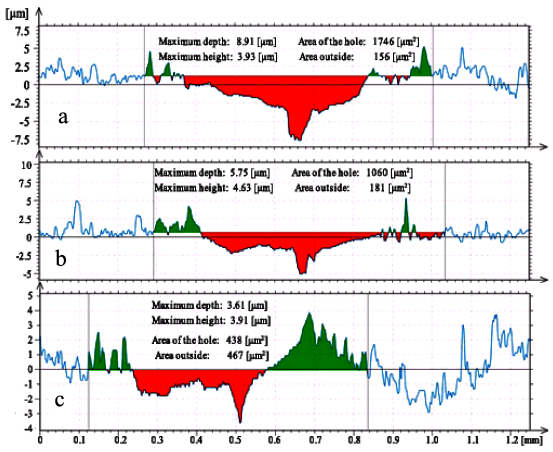

Fig. 5. The results of wear resistance tests obtained by scratch tester REVETEST of samples (Ti, Hf, Nb, Si)N: (a) after annealing 500 °C, (b) after annealing 800 °C, (c) after annealing 1000 °C.

stresses, and perhaps this is also associated with an increase of friction coefficient (although as can be seen from the results of EDX analysis there is an oxide film with thickness of 60–75 nm) [15, 17, 20–24].

4. Conclusions

It was shown that high temperature treatment leads to significant increase of the nanocrystallites size of the solid solutions from 3 nm to 7.7 nm. Also, annealing leads to recrystallization processes.

High values of macro- and microdeformations in coatings are considered to occur due to an "atomic peening" effect, which results to non-ordered distribution of titanium atoms implanted to the film during its growth.

Thermal annealing at temperatures to 1000 °C leads to an abrupt relaxation of compression stress of the coatings. This is accompanied by decrease of lattice parameters, and by deformation of lattice by packing defects in a metallic sublattice of (Ti, Hf)N, (Ti, Nb)N solid solutions.

Acknowledgments

The work was done under financial support of Ministry of Education and Science of Ukraine (state program, order No. 411), and in collaboration with NIMS (Tsukuba, Japan) and Martin Luther University (Dresden, Germany). The work was supported by Ministry of Education and Science of Ukraine (project No 0112U005920) and Ministry of Education and Science of Russia (grant No. 12-08-31060).

References

[1] A.D. Pogrebnjak, A.G. Ponomarev, A.P. Shpak, Yu.A. Kunitskii, *Phys. Usp.* **55**, 270 (2012).

[2] A.D. Pogrebnjak, A.P. Shpak, N.A. Azarenkov, V.M. Beresnev, *Phys. Usp.* **52**, 29 (2009).

[3] A.D. Pogrebnjak, E.A. Bazyl, *Vacuum* **64**, 1 (2001).

[4] A.D. Pogrebnyak, V.M. Beresnev, D.A. Kolesnikov, M.V. Kaverin, A.P. Shypylenko, K. Oyoshi, Y. Takeda, R. Krause-Rehberg, A.G. Ponamarev, *Tech. Phys. Lett.* **39**, 280 (2013).

[5] A.D. Pogrebnjak, O.V. Sobol, V.M. Beresnev, P.V. Turbin, G.V. Kirik, N.A. Makhmudov, M.V. Il'yashenko, A.P. Shypylenko, M.V. Kaverin, M.Yu. Tashmetov, A.V. Pshyk, *Nanostruct. Mater. Nanotechnol. IV: Ceram. Eng. Sci. Proc.* **31**, 127 (2010).

[6] O.V. Sobol, A.D. Pogrebnyak, V.M. Beresnev, *Phys. Met. Metallogr.* **112**, 199 (2011).

[7] J. Musil, J. Vicek, P. Zeman, *Adv. Appl. Ceram.* **107**, 148 (2008).

[8] A.D. Korotaev, V.D. Borisov, V.Y. Moshkov, S.V. Ovchinnikov, J.P. Pinzhin, A.N. Tyumentsev, *Phys. Mesomech.* **12**, 269 (2009).

[9] A.D. Pogrebnjak, V.M. Beresnev, A.A. Demianenko, V.S. Baidak, F.F. Komarov, M.V. Kaverin, N.A. Makhmudov, D.A. Kolesnikov, *Phys. Solid State* **54**, 1882 (2012).

[10] O.V. Sobol, A.A. Andreev, V.F. Gorban, N. Krapivka, V.A. Pole, I.V. Serdyuk, V.E. Filchikov, *Tech. Phys. Lett.* **38**, 616 (2012).

[11] A. Vladescu, C.M. Cotrut, A. Kiss, M. Balaceanu, V. Braic, S. Zamfir, M. Braic, *U.P.B. Sci. Bull., Series B* **68**, 57 (2006).

[12] O.V. Sobol', A.A. Andreev, S.N. Grigoriev, M.A. Volosova, V.F. Gorban', *Met. Sci. Heat Treat* **54**, 28 (2012).

[13] A. Öztürk, K.V. Ezirmik, K. Kazmanli, M. Ürgen, O.L. Eryilmaz, A. Erdemir, *Tribol. Int.* **41**, 49 (2008).

[14] D. Pakula, L.A. Dobrzanski, A. Kriz, M. Staszuk, *Arch. Mater. Sci. Eng.* **6**, 53 (2010).

[15] A.D. Pogrebnjak, O.V. Bondar, O.V. Sobol, V.M. Beresnev, *Soft Nanosci. Lett.* **3**, 46 (2013).

[16] I.V. Blinkov, S.A. Volkhonsky, V.N. Anikin, M.I. Petrzhik, D.E. Derevtsova, *Phys. Chem. Mater. Proc.* **4**, 37 (2010) (in Russian).

[17] T.N. Kołtunowicz, P.V. Zhukowski, V.V. Fedotova, A.M. Saad, A.V. Larkin, A.K. Fedotov, *Acta Phys. Pol. A* **120**, 35 (2011).

[18] T.N. Kołtunowicz, P. Zhukowski, V.V. Fedotova, A.M. Saad, A.K. Fedotov, *Acta Phys. Pol. A* **120**, 39 (2011).

[19] Sh.-Y. Lin, Sh.-Y. Chang, Y.-Ch. Huang, F.-Sh. Shieu, J.-W. Yeh, *Surf. Coat. Technol.* **206**, 5096 (2012).

[20] J. Musil, *Surf. Coat. Technol.* **207**, 50 (2012).

[21] A.D. Pogrebnjak, A.P. Shpak, V.M. Beresnev, D.A. Kolesnikov, Yu.A. Kunitsky, O.V. Sobol, V.V. Uglov, F.F. Komarov, A.P. Shypylenko, A.A. Demyanenko, V.S. Baidak, V.V. Grudnitskii, *J. Nanosci. Nanotechnol.* **12**, 9213 (2012).

[22] S.V. Rempel, A. Gusev, *JETP Lett.* **88**, 508 (2008).

[23] A.I. Gusev, *Nanomaterials, Nanostructures and Nanotechnology*, Fizmatlit, Moscow 2005.

[24] A.V. Khomenko, N.V. Prodanov, *Condens. Matter Phys.* **11**, 615 (2008).